

Two-Dimensional Measurements of Velocity Using Two Rotating Gratings

J. Ritonga, T. Ushizaka, and T. Asakura

Research Institute of Applied Electricity, Hokkaido University,
Sapporo, Hokkaido 060, Japan

Received 10 October 1988/Accepted 9 January 1989

Abstract. A two-dimensional vector velocimeter is proposed on the basis of the time-varying spatial filtering method using a rotating disk with two transmission gratings. The filtering characteristics of the spatial filter used in the velocimeter were studied theoretically. A preliminary experiment was performed to measure the velocity vector of a rotating random pattern. The experimental results show the usefulness of the present velocimeter for measurements of the velocity.

PACS: 07.60, 42.80

Optical velocimetry [1] using a spatial filter is useful for measurements of the local instantaneous velocity in the fluid and the object motion without disturbance of them. In this field, laser Doppler velocimetry has been well known to be advantageous for measuring the flow or moving velocity. However, the optical system is much simpler and more stable in optical velocimetry with the spatial filter than in laser Doppler velocimetry.

Gaster [2] applied the spatial filtering method using a transmission grating to measurements of the velocity in the liquid flow. Ushizaka and Asakura [3] verified its usefulness in a microscopic region by applying Gaster's method to measurements of the flow velocity in a small glass tube. Nevertheless, the transmission grating method has a deficiency in the directional ambiguity which is usually insignificant for the flow or the motion whose velocity direction is known beforehand. However, the direction of the flow velocity is generally unknown in a rapidly flowing fluid or a recirculating flow. In such a case, the flow direction has to be determined by the spatial filtering method. Several methods to determine the flow direction have already been proposed on the basis of the phase relation between the output signals. Slaaf et al. [4] proposed the three-stage prism grating method in which the phase relations between the three signals obtained by using the prism grating and the three

photodetectors are used to determine the direction of the velocity. In the method of Aizu et al. [5], the direction of the flow is discriminated from the phase relation between the two output signals obtained from the two photodetectors placed behind two transmission gratings. The above phase-relation techniques are only suitable for eliminating the directional ambiguity in measurements of the flow velocity.

Compared with the above methods, the method [2] based on the frequency shifting technique using the moving gratings is of greater interest for measurements of the flow direction. The frequency shifting technique has also been used in laser Doppler velocimetry on the basis of the different principles, for example, using a moving diffraction grating [6] and an acousto-optic Bragg cell [7]. Itakura et al. [8] proposed the two-stage grating velocimetry based on the frequency shifting technique using a liquid crystal cell array. In their method, the liquid crystal cell array acts as a spatio-temporal spatial filter with a moving transmission grating which produces the frequency shift. Their method based on the frequency shifting technique is able to determine not only the forward and backward directions of the velocity but also any direction of the velocity from 0° to 360° . However, the frequency shifting technique using the liquid crystal cell array is not adequate for rapidly moving objects because of its relatively poor frequency response.

Gaster [2] proposed the two-dimensional vector velocimetry based on the frequency shifting technique using rotating radial gratings. In his method, however, it is necessary to mechanically rotate the two disk gratings. For this reason, the system becomes complicated and unstable.

The new method proposed here uses the frequency shifting technique employing a rotating disk with two transmission gratings which are set perpendicularly to each other in their grids on the disk. Based on the principle of the spatial filtering method, each grating extracts the vector component of the velocity in a direction perpendicular to the grating grids. The frequency response of the new method depends mainly on a rotation rate of the disk with gratings. Therefore, the method is applicable for measurements of a wide range of velocities for which the rotation rate of the grating disk can be easily varied. Preliminary experiments have been conducted to measure the absolute value and the direction of the velocity of a random pattern on the rotating disk. The experimental results verify the usefulness of the proposed method.

1. Principle of the Method

1.1. Construction of the System

Figure 1 shows schematically the new system for measurements of the velocity components using a rotating disk with two transmission gratings. When the probing region is illuminated by the focused light, the illuminating light is scattered by an object existing in that region. By means of a lens L_1 , the scattered light forms an image of the object at a mask M which has a pinhole to define the probe volume. The light passing through the mask M forms the two object images on the moving gratings G_x and G_y by means of a relay lens L_2 and a beam splitter BS . The gratings are set perpendicularly to each other in their grids and are connected to the orthogonal components of the object velocity. The light passing through the two gratings is collected by a lens L_3 and fed to the photodetector PD .

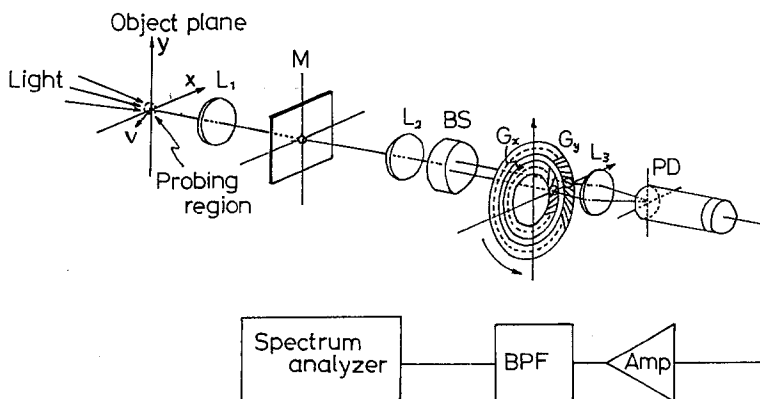


Fig. 1. Schematic diagram of the system for measurements of the velocity components using a rotating disk with two gratings

When the object images move over the two moving gratings, two periodic signals are generated from the photodetector. The signals, after amplification and passing through an appropriate band-pass filter BPF, are analyzed by means of a spectrum analyzer. The frequencies of the two periodic signals analyzed by the spectrum analyzer are related to the object velocity v_o and the shifting velocity v_g due to the moving gratings. The orthogonal components v_{ix} and v_{iy} of the image velocity vector v_i are determined from the frequencies of the signals, if the interval p of grating grids and the magnification M of the optical system are known beforehand. The absolute velocity $|v_o|$ and the direction θ of the moving object are determined from the relations of $|v_o| = (1/M)(v_{ix}^2 + v_{iy}^2)^{1/2}$ and $\theta = \tan^{-1}(v_{iy}/v_{ix})$.

1.2. Configuration of the Rotating Gratings

Figure 2(a) shows the configuration of the rotating gratings which were drawn on a circular transparent disk by a computer through the plotter. The imaging regions on the two gratings are magnified in Fig. 2b.

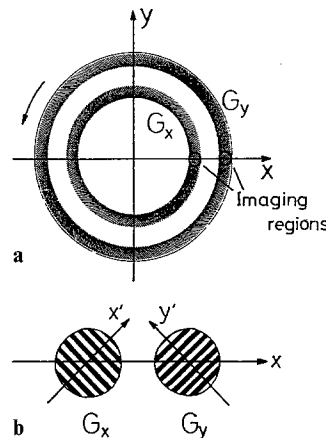


Fig. 2a, b. Configuration of the rotating disk gratings for measurements of the velocity components: **a** the rotating disk gratings and **b** magnified patterns of the two imaging regions in **a**

The grid of the inner grating G_x lies perpendicular to that of the outer grating G_y , and the two gratings are made to have the same spatial period p . The grids of the gratings in the imaging regions may be assumed to be parallel because the radii of the two areas where both gratings are drawn are much bigger than the radii of the circular imaging regions. The disk is rotated by an electric motor to produce the frequency shifts for the light passing through the two moving gratings.

1.3. Determination of the Absolute Value and the Direction of the Velocity

In Fig. 2, the x' and y' coordinates are set at the plane of the gratings G_x and G_y because each grating detects the velocity components which are perpendicular to the grating grids. In order to determine the velocity components, it is important to note by referring to Fig. 1 that the x' and y' coordinates on the gratings are generally different from the x and y coordinates at the object plane where the flow or the moving object is located. In the present system, the x' and y' coordinates are set to be inclined by an angle of 45° to the x and y coordinates (refer to Fig. 2).

Figure 3 indicates the relation between the image velocity vector \mathbf{v}_i and the grating velocity vector \mathbf{v}_g . In the figure, the velocity vector \mathbf{v} corresponds to the relative velocity of the image velocity vector \mathbf{v}_i with respect to the velocity vector \mathbf{v}_g of the grating. In the coordinate system (x', y') , the image velocity vector \mathbf{v}_i has the components $v_{ix'}$ and $v_{iy'}$, and the velocity vector \mathbf{v}_g of the grating has the components $v_{gx'}$ and $v_{gy'}$. The relation between the vectors \mathbf{v} , \mathbf{v}_i , and \mathbf{v}_g is given by

$$\mathbf{v} = \mathbf{v}_i + \mathbf{v}_g. \quad (1)$$

In this case, the velocity vector \mathbf{v}_i is at an angle θ' to the x' axis and an angle θ to the x axis. The angles θ and θ'

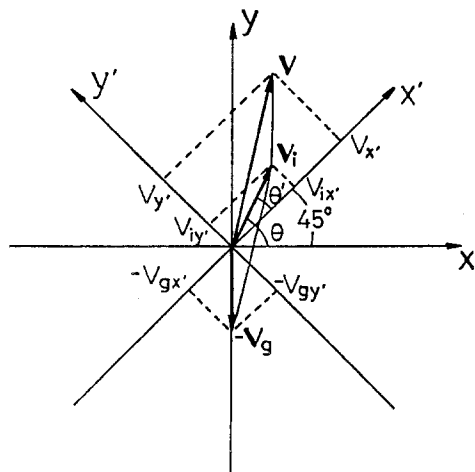


Fig. 3. Relations between the image velocity vector \mathbf{v}_i , the grating velocity vector \mathbf{v}_g , and the relative velocity vector \mathbf{v} in the coordinate systems (x, y) and (x', y')

are related by

$$\theta = \theta' + 45^\circ. \quad (2)$$

By measuring the components v_x and v_y of the relative velocity vector \mathbf{v} at the x' and y' coordinates, the components $v_{ix'}$ and $v_{iy'}$ of the image velocity vector can be determined from relation (1) as

$$\begin{aligned} v_{ix'} &= v_x - v_{gx'}, \\ v_{iy'} &= v_y - v_{gy'}. \end{aligned} \quad (3)$$

Furthermore, the direction of the image velocity vector \mathbf{v}_i at the x' and y' coordinates is given by

$$\theta' = \tan^{-1} \left(\frac{v_{iy'} - v_{gy'}}{v_{ix'} - v_{gx'}} \right). \quad (4)$$

The components of the image velocity are related by $v_x = pf_{x'}$ and $v_y = pf_{y'}$ to the spatial period p of the grating grids and the frequency components, $f_{x'}$ and $f_{y'}$, of actual output signals relating to the relative velocity \mathbf{v} of the image. On the other hand, the components of the grating velocity behave as $v_{gx'} = pf_{gx'}$ and $v_{gy'} = pf_{gy'}$ with the frequency components $f_{gx'}$ and $f_{gy'}$ of the output signals relating to the velocity of the gratings which can be obtained when the object does not move. The frequency components $f_{gx'}$ and $f_{gy'}$ correspond to the shifting frequencies of the moving gratings G_x and G_y , respectively.

The direction of the image (or object) velocity vector at the coordinate point (x, y) can be finally obtained from (2) and (4) as

$$\theta = \tan^{-1} \left(\frac{\Delta f_{y'}}{\Delta f_{x'}} \right) + 45^\circ, \quad (5a)$$

where

$$\begin{aligned} f_{ix'} &= \Delta f_{x'} = f_{x'} - f_{gx'}, \\ f_{iy'} &= \Delta f_{y'} = f_{y'} - f_{gy'}. \end{aligned} \quad (5b)$$

The signs of $f_{x'}$ and $f_{y'}$ in (5) play an important role in determining the forward and backward directions of the image velocity. A plus or minus sign depends on the relative relationship between the velocities of the image and the gratings.

On the basis of (3), the absolute value of the image velocity vector can be given by

$$|\mathbf{v}_i| = p(\Delta f_{x'}^2 + \Delta f_{y'}^2)^{1/2}, \quad (6)$$

which is related by $|\mathbf{v}_o| = |\mathbf{v}_i|/M$ to the absolute value $|\mathbf{v}_o|$ of the object velocity.

2. Signal Analysis

We are now in a position to study theoretically the effect of the moving gratings on the output signals to be obtained from the photodetector. As indicated in

Figs. 1 and 2, the coordinate system (x', y') is set in the plane of the transmission gratings. Let the light transmittance of the grating G_x (or G_y) and the light intensity of the object image at the plane of the grating be $h(x', y')$ and $o(x', y')$, respectively. When the image moves with velocity $v_{ix'}$ along the x' axis on the grating G_x which is also moving with the velocity $v_{gx'}$, all the light passing through the grating G_x is received by the photodetector PD. The time-varying output signal $g_x(t)$ from the photodetector can be represented by

$$g_x(t) = K \iint_{-\infty}^{\infty} o(x' - v_{ix'}t, y') h(x', y'; t) dx' dy', \quad (7)$$

where K is a constant and $h(x', y'; t)$ indicates the shifting behavior of the grating G_x which is described by

$$h(x', y'; t) = m(x', y') h(x' - v_{gx'}t, y') \quad (8)$$

in which $m(x', y')$ denotes the transmission function of the mask restricting spatially the view of the grating G_x . For simplicity, it is assumed that the grating and the mask have transmittances with sinusoidal and gaussian amplitudes, respectively. Equation (8) then becomes

$$h(x', y', t) = \frac{1}{2} \exp\left(-\frac{x'^2 + y'^2}{2Q^2}\right) \times \left\{1 + \cos\frac{2\pi}{p}(x' - v_{gx'}t)\right\}, \quad (9)$$

where $2Q$ indicates the effective size of the mask and p is again the spatial period of the grating. By assuming that the intensity $o(x', y')$ of the object image in (7) follows a stationary random process and by applying, therefore, the Wiener-Khinchin theorem to the autocorrelation of the output signal $g_x(t)$, the power spectral density function (or power spectrum) $G(f_{x'})$ of the time-varying output signal $g_x(t)$, which can be actually measured, takes the form:

$$G(f_{x'}) = \frac{K}{v_{ix'}} \int_{-\infty}^{\infty} O\left(\frac{f_{x'} - v_{gx'}/p}{v_{ix'}}, v\right) \times \left|H\left\{\frac{f_{x'} + (v_{ix'} - v_{gx'})/p}{v_{ix'}}, v\right\}\right|^2 dv, \quad (10)$$

where $O(\dots)$ and $H(\dots)$ correspond to the power spectrum of the intensity distribution $o(x', y')$ and the Fourier spectrum of the transmittance $h(x', y'; t)$ of the grating with the mask. If the average size of the object image is sufficiently small compared with both the size of the probing region and the spatial period of the gratings, the power spectrum $O(\dots)$ can be set to unity under the white noise approximation. Then, the characteristic of the power spectrum $G(f_{x'})$ can be investigated only from the power spectrum $|H(\dots)|^2$ of the

grating. By substituting the power spectrum of (9) into (10), and by performing the integration with respect to v , the power spectrum of the output signal is obtained as

$$G(f_{x'}) = \frac{K(\pi Q)^2}{v_{ix'}} [\exp\{- (n\pi f_{x'}/\Delta f_{x'})^2\} + \exp\{- (n\pi/\Delta f_{x'})^2 [f_{x'} - (f_{gx'} - \Delta f_{x'})]^2\} + \exp\{- (n\pi/\Delta f_{x'})^2 [f_{x'} + (f_{gx'} - \Delta f_{x'})]^2\}], \quad (11)$$

where n is the number of grating grids within the mask, which is given by $n = 2Q/p$, and $f_{x'} = v_{x'}/p$.

The central frequency of the power spectrum in the positive side along the x' axis is given from (11) as

$$f_{x'} = f_{gx'} - \Delta f_{x'} = f_{gx'} - v_{ix'}/p, \quad (12)$$

where $f_{gx'} = v_{gx'}/p$ corresponds to the shifting frequency of the grating G_x which can be obtained when the object does not move. A discussion based on equations (7) to (12) can likewise be given for the output signal $g_y(t)$ obtained through the grating G_y . Finally, the central frequency of the output signal $g_y(t)$ with respect to the positive side along the y' axis is given by

$$f_{y'} = f_{gy'} - \Delta f_{y'} = f_{gy'} - v_{iy'}/p, \quad (13)$$

where $f_{gy'} = v_{gy'}/p$ corresponds to the shifting frequency of the grating G_y .

Figure 4 shows the theoretical results of the power spectra obtained from (11) for the number $n = 8$ of grating grids in the mask, the frequency $f_{x'} = 0.2$ kHz of the relative image velocity, and the frequency shift $f_{gx'} = 1$ kHz due to the grating movement. Figure 4a shows that, when the grating does not move ($f_{gx'} = 0$), the central frequency $f_{x'} = 0.2$ kHz of the output signal appears near the pedestal frequency component. Figures 4b and 4c show that the central frequency $f_{x'}$ is shifted to the high and low frequency sides from the frequency $f_{gx'}$ shifted by the moving grating when the image moves in two opposite backward and forward directions. In other words, Fig. 4b indicates the case where the grating and the image move in opposite directions, while in Fig. 4c the grating and the image move in the same direction. As a result, the signal components with respect to the velocity components of the moving object are produced near the shifting frequency of the grating. This means that the output signal in the spectral domain is transferred to the high frequency by using the rotating gratings. Therefore, the undesired pedestal signal appearing around the zero frequency does not affect the desired signals to be obtained. Consequently, the pedestal signal can be easily removed because of the frequency interval introduced between the required signal and the pedestal signal. By means of the two gratings G_x and G_y ,

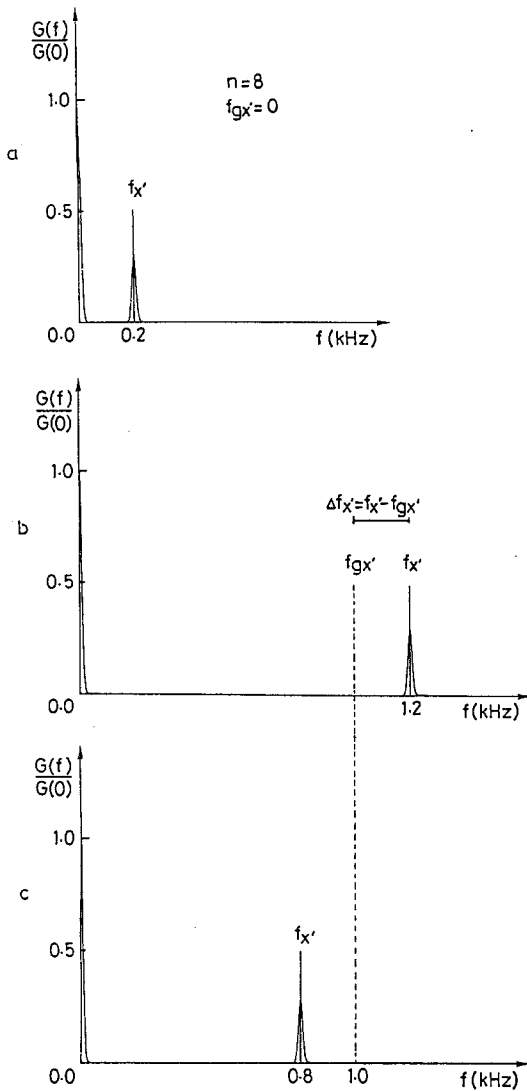


Fig. 4a-c. Power spectra of the output signals obtained from (11): **a** only the movement of the image, **b** movement of the grating and the image in opposite directions, and **c** movement of the grating and the image in the same direction

which are set perpendicularly to each other, the orthogonal components of the velocity vector can be measured. Thereby, the direction and the absolute value of the velocity vector are determined from (5) and (6), respectively.

3. Experimental Results and Discussion

By using the experimental setup of Fig. 1, the preliminary experiment was performed to measure the velocity vector of a random pattern on the rotating disk. The inner and outer gratings shown in Fig. 2a have grid numbers of $N = 266$ and $N = 400$ with radii of 4.13 cm and 6.2 cm. Under these conditions, the two gratings have the same spatial period of 0.974 mm. The grids of

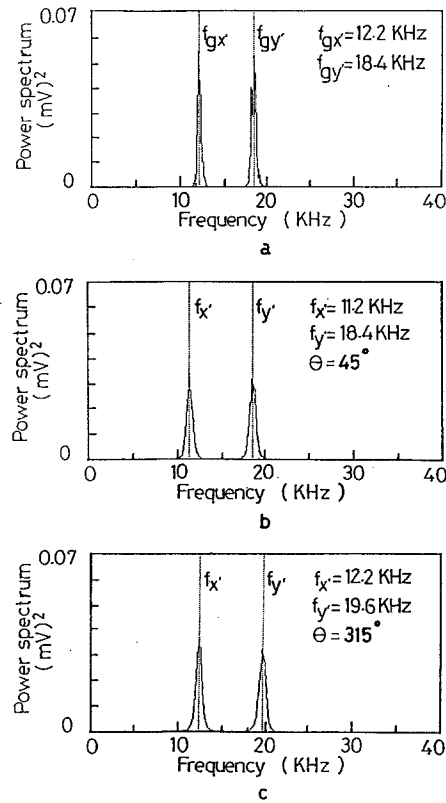


Fig. 5a-c. Power spectra of the output signals obtained experimentally with the shifting frequencies of the gratings G_x and G_y : **a** movement of the gratings only, **b** movement of the object in the direction $\theta = 45^\circ$ together with the movement of the gratings, **c** movement of the object in the direction $\theta = 315^\circ$ together with movement of the gratings

both gratings in the imaging region were assumed to be parallel because the radii of both gratings are much bigger than the radii of the imaging region on the gratings.

The relay optics consisting of the lens L_2 and the beam splitter BS is set to have a magnification of one and an aperture diameter of 2 mm. The effective spatial period p of grating grids is 0.688 mm and the direction of the grating grids has an inclination of 45° to the direction of the circumference. The disk is rotated at 2760 rpm which produces the frequency shifts of 12.2 kHz and 18.4 kHz for the inner and outer gratings, respectively.

Figure 5a shows the power spectra of the rotating gratings G_x and G_y with the frequencies $f_{gx} = 12.2$ kHz and $f_{gy} = 18.4$ kHz, respectively. These frequencies were obtained from the rotating gratings under the condition that the object does not move. In the experiment, these frequencies were used to shift the frequencies of the actually obtained output signals. Figures 5b and c show the power spectra of actual output signals after passing through the electric filters in the signal-analyzing system. Figure 5b shows the

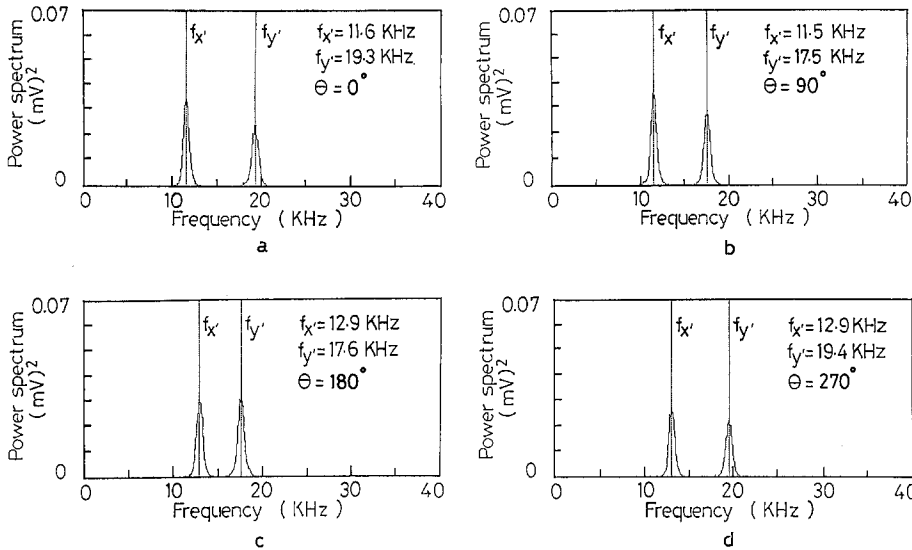


Fig. 6a-d. Power spectra of the output signals obtained experimentally with the shifting frequencies of the gratings: the movement of the object is in the directions $\theta = a$ 0° , b 90° , c 180° , d 270°

power spectra of the output signal when the object moves in the direction of $\theta = 45^\circ$ (in the counter-clockwise direction) with respect to the x and y coordinates. In this case, the object image moves along the x' axis on the grating G_x . The central frequency $f_{x'}$ of the output signal shifted by the frequency of the grating G_x is 11.2 kHz, while no further shift is produced for the frequency $f_{y'}$ from the frequency shifted by the grating G_y . On the other hand, Fig. 5c shows the power spectra of the output signal when the object moves in the direction of $\theta = 315^\circ$. In this case, the object image moves along the y' axis on the grating G_y . As is seen in Fig. 5c, the central frequency $f_{y'}$ is further shifted by 19.6 kHz from the frequency shifted by the grating G_y , but no further shift is produced for the frequency $f_{x'}$ from the frequency shifted by the grating G_x .

Figure 6 shows the power spectra of output signals when the object image moves across both gratings G_x and G_y . In this case, the image has two velocity components with respect to the x' and y' coordinates at the image plane over the gratings. Figure 6a-d correspond to the cases that the image (or object) was moving in the four directions of $\theta = 0^\circ, 90^\circ, 180^\circ$, and 270° with a pair of the central frequencies $f_{x'}$ and $f_{y'}$ at 11.6 and 19.3 kHz, 11.5 and 17.5 kHz, 12.9 and 17.6 kHz, and 12.9 and 19.4 kHz, respectively. The frequencies for the true velocity components of the image are determined by subtracting the frequencies obtained from actual output signals from the originally shifted frequencies.

Figure 7 shows the normalized absolute value and the direction of the object velocity which were drawn in the polar coordinates where the direction and the absolute value of the velocities were evaluated from (5) and (6). The dark circles and the solid lines indicate the

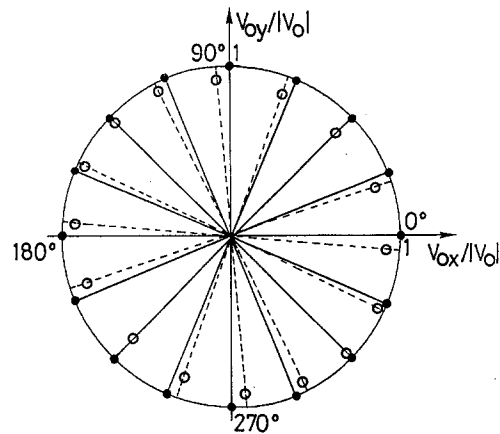


Fig. 7. Comparison of the normalized absolute values and the directions of the object velocity actually measured at the object plane and those obtained from measurements of the central frequencies of output signals

absolute values and the directions of the actual object velocity. The open circles and the dashed lines indicate the absolute values and the directions of the object velocity determined from measurements of the central frequencies. Figure 7 shows that the absolute values and the directions of the object velocity determined from frequency measurements of the output signals are slightly different from those of the object velocity obtained from actual measurements at the object plane. The discrepancy is less than 7%. The gratings themselves may cause this error in measuring the frequency components of the velocity vector because the gratings prepared in our laboratory may not be sufficiently accurate. Equation (5b) indicates that the frequency components $f_{x'}$ and $f_{y'}$ of the relative image velocity depend on the shifted frequencies $f_{gx'}$ and $f_{gy'}$ of both gratings. An error can be clearly seen from the

power spectrum of the grating G_y in Fig. 5a. The grating G_y produces a frequency shift of 18.4 kHz. However, the two peaks can be observed for the frequency $f_{gy'}$ with the band-width of 2 kHz. One of the two peak frequencies may be considered to produce an error of the frequency $f_{gy'}$. The error in the frequency shift does not come from mechanical vibration because the grating was rotated by the electric motor. But it may come from the spatial period of the grating itself because the grating was originally drawn by a plotter. For example, a plotter with an accuracy of 0.1 mm cannot accurately draw the 400 slits of the grating with the spatial period of $p=0.974$ mm at the radii of 62 mm. Therefore, the inhomogeneity of the spatial period of the gratings and the discontinuity inevitably produced when the two ends of the gratings are joined may be considered to produce the error in the frequency shifting.

4. Conclusion

A new method utilizing a pair of perpendicular gratings in a rotating disk is proposed for measurements of

the velocity vector. It is able to measure the vector quantity of the object velocity because the two components of the velocity vector can be obtained simultaneously. The frequency response of the method depends mainly on the rate of rotation of the disk gratings. Therefore, the proposed method is applicable for measurements of the velocity with a wide variety of speeds and is expected to be used for measurements of the object velocity with solid and fluid conditions in macroscopic and microscopic regions.

References

1. Y. Aizu, T. Asakura: *Appl. Phys. B* **43**, 209 (1987)
2. M. Gaster: *J. Fluid Mech.* **20**, 183 (1964)
3. T. Ushizaka, T. Asakura: *Appl. Opt.* **22**, 1870 (1983)
4. D.W. Slaaf, J.P.S.M. Rood, G.J. Tangelder, T.J.M. Jeurens, R. Alewijnse, R.S. Reneman, *T. Arts: Microvasc. Res.* **22**, 110 (1981)
5. Y. Aizu, T. Ushizaka, T. Asakura: *Appl. Opt.* **24**, 636 (1985)
6. M.K. Mazumder: *Appl. Phys. Lett.* **16**, 462 (1970)
7. W.M. Farmer, J.O. Hornkorl: *Appl. Opt.* **12**, 2636 (1973)
8. Y. Itakura, A. Sugimura, S. Tsutsumi: *Appl. Opt.* **20**, 2819 (1981)